Supplementary information for:

Thermally activated delayed fluorescent (TADF) photocatalysts: mechanistic understanding and accessible tools to quantify quenching rate constants of their lowest S_1 and T_1 excited states

Federica Fina, Caterina Bellatreccia, Xia Wu, Pier Giorgio Cozzi, Alessandro Troisi, Sergei Vinogradov and Paola Ceroni

Table of contents

General methods

All reagents, solvents and chemicals were purchased from Sigma-Aldrich, Fisher, or Alfa-Aesar and used directly unless otherwise stated (purity: reagent or analytical grade).

Photophysical measurements: Emission spectra at 77 K were registered on a Perkin Elmer LS55 fluorometer in fluorescence mode and phosphorescence mode with gate time of 7 ms and delay time of 0.5 ms in butyronitrile rigid matrix; Fluorescence lifetimes shorter than 10 μs were measured with an Edinburgh FLS1000 or an Edinburgh FLS920 spectrofluorometer equipped with a TCC900 card for data acquisition in time-correlated single-photon counting experiments (0.5 ns time resolution) with a 405 nm LASER. Longer lifetimes were measured by the above-mentioned FLS1000 fluorimeter equipped with a microsecond flashlamp. Time-resolved PL measurements were fitted to an exponential decay model, using the EI FLS980 or Edinburgh FLS920 software. The estimated experimental errors are: 2 nm on the band maxima, 5% on the luminescence lifetime, 15% on the experimentally determined kinetic quenching constants.

Cyclic voltammetry was performed using a PGSTAT302N (Metrohm) potentiostat. The measurement was performed in Argon saturated dichloromethane solution containing the analyte (0.5 mM) and $TBAPF_6$ (0.1 M) as a supporting electrolyte and a scan rate 200 $mV \cdot s^{-1}$. DCM was used instead of toluene because with the latter the cell resistance is high because toluene does not allow sufficient dissolution of the electrolytic salt. The electrochemical cell was assembled with a glassy carbon working electrode (3 mm diameter), Pt wire as counter electrode, Ag wire as a quasi reference electrode and Fc as internal standard (Fc^+/Fc= +0.39 V vs. SCE) The supporting electrolyte was dried under vacuum at 100 °C overnight prior to use.

Kinetic simulations: Our kinetic simulation consists in a C-language code, which numerically calculates the evolution of $[S_0]$, $[S_1]$, $[T_1]$, [Q], $[Q^+]$ according to the following differential equations:

$$\frac{d[S_1]}{dt} = k_{risc}[T_1] - (k_{S1\rightarrow S0} + k_{isc} + k_{qS}[Q])[S_1] \quad \text{(S1)}$$

$$\frac{d[T_1]}{dt} = k_{isc}[S_1] - (k_{T1\rightarrow S0} + k_{risc} + k_{qT}[Q])[T_1] \quad \text{(S2)}$$

$$\frac{d[Q]}{dt} = -(k_{qS}[S_1] + k_{qT}[T_1])[Q] \quad \text{(S3)}$$

$$\frac{d[Q^+]}{dt} = (k_{qS}[S_1] + k_{qT}[T_1])[Q] \quad \text{(S4)}$$

$$\frac{d[S_0]}{dt} = (k_{S1\rightarrow S0} + k_{qS}[Q])[S_1] + (k_{T1\rightarrow S0} + k_{qT}[Q])[T_1] \quad \text{(S5)}$$

where $k_{S1\rightarrow S0}$ and $k_{T1\rightarrow S0}$ are illustrated in Figure S1 and can be related to the kinetic constants in Figure 1 as follows:

$$k_{S1\rightarrow S0} = k^S + k_{isc} \quad \text{(S6)}$$

$$k_{T1\rightarrow S0} = k^T + k_{risc} \quad \text{(S7)}$$

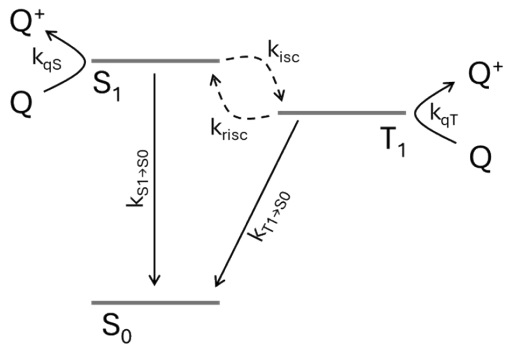

Figure S1: Kinetic constant notation used in supporting information for this work.

The following starting conditions were employed in all simulated data:

$$[S_0](t=0) = 1\text{mM}$$

$$[S_1](t=0) = 0.01\text{mM}$$

$$[T_1](t=0) = [Q^+](t=0) = 0\ \text{mM}$$

$$[Q](t=0)\ \text{variable}$$

The timestep of the simulation is set at 1 ps in order to obtain extremely precise datasets.

A "simulated decay" is defined as a kinetic trace generated with the aforementioned simulation of either $[S_0]$, $[S_1]$, $[T_1]$, $[Q]$, $[Q^+]$, given a certain set of kinetic constants and a certain initial concentration of the quencher ($[Q]$) (input parameters).

All $[S_1]$ simulated decays were fitted with a biexponential decaying function with the following general formula:

$$[S_1] = A_1 e^{-t/\tau_{1S}} + A_2 e^{-t/\tau_{2S}} \quad \text{(S8)}$$

All $[T_1]$ simulated decays were fitted with a biexponential function with the following general formula:

$$[T_1] = -Be^{-t/\tau_{1T}} + Be^{-t/\tau_{2T}} \quad \text{(S9)}$$

Therefore, A_1, A_2, B, τ_{1S}, τ_{2S}, τ_{1T} and τ_{2T} are output values that can be compared to the pre-exponential factors and τ_p and τ_d lifetimes predicted by the exact solutions based on the input parameters used for the simulated decay under analysis (eq 1-4).

A "simulated SV experiment" is defined as a set of simulated decays that have the same set of kinetic constants but differ for the initial [Q].

Computational methods: All density functional theory (DFT), time-dependent DFT (TD-DFT) and unrestricted DFT (UDFT) calculations were carried out using the Gaussian 16A suite of programs, adapting a protocol previously used to screen a large number of organic compounds and validated against experimental data.[1-2] Geometry optimizations were carried out at the BLYP35/def2svp level and the corresponding TD-DFT calculations were utilizing the M06-2X/def2svp level of theory.[3] Solvation effects were all taken into account using toluene based on the polarizable continuum model (PCM).[4] This methodology exhibits a linear

calibration correction between computational and experimental excited state energies and has been used in previous studies.[5] Multiwfn was used to analyze the hole and electron distribution.[6]

Experimental data

Kinetic simulation

Table S1: Summary of the lifetimes (τ_{1S}, τ_{2S}, τ_{1T}, τ_{2T}) obtained from the fitting of the simulated decays with equations S8, S9 upon variation of all kinetic constants over 3 orders of magnitude. For clarity, in each experiment the kinetic constant which is varied with respect to the first experiment is marked in red. For each set of kinetic constants, we performed a simulated Stern-Volmer experiment, with increasing concentrations of the quencher Q. The columns τ_{2S} and τ_{2T} are highlighted in green to show that the delayed lifetime of the singlet and the decaying lifetime of the triplet are coincident under all the conditions explored.

exp	$k_{S1\rightarrow S0}$ / s^{-1}	k_{isc} / s^{-1}	k_{risc} / s^{-1}	$k_{T1\rightarrow S0}$ / s^{-1}	k_{qS} / $s^{-1}M^{-1}$	k_{qT} / $s^{-1}M^{-1}$	[Q] / M	τ_{1S} / s	τ_{2S} / s	τ_{1T} / s	τ_{2T} / s
1_0							0	2E-09	2.50E-05	2E-09	2.50E-05
1_1							1E-03	2E-09	1.86E-06	2E-09	1.86E-06
1_2	3E8	2E8	5E4	1E4	5E8	5E8	3E-03	1.99E-09	6.50E-07	1.99E-09	6.50E-07
1_3							6E-03	1.99E-09	3.29E-07	1.99E-09	3.29E-07
1_4							9E-03	1.98E-09	2.20E-07	1.98E-09	2.20E-07
2_0							0	3.12E-10	1.76E-05	3.12E-10	1.76E-05
2_1							1E-03	3.12E-10	1.80E-06	3.12E-10	1.80E-06
2_2	3E9	2E8	5E4	1E4	5E8	5E8	3E-03	3.12E-10	6.42E-07	3.12E-10	6.42E-07
2_3							6E-03	3.12E-10	3.27E-07	3.12E-10	3.27E-07
2_4							9E-03	3.12E-10	2.19E-07	3.12E-10	2.19E-07
3_0							0	4.35E-09	6.05E-05	4.35E-09	6.05E-05
3_1							1E-03	4.34E-09	1.94E-06	4.33E-09	1.94E-06
3_2	3E7	2E8	5E4	1E4	5E8	5E8	3E-03	4.32E-09	6.60E-07	4.31E-09	6.60E-07
3_3							6E-03	4.29E-09	3.32E-07	4.29E-09	3.32E-07
3_4							9E-03	4.26E-09	2.22E-07	4.26E-09	2.22E-07
4_0							0	4.34E-10	6.05E-05	4.34E-10	6.05E-05
4_1							1E-03	4.34E-10	1.94E-06	4.33E-10	1.94E-06
4_2	3E8	2E9	5E4	1E4	5E8	5E8	3E-03	4.34E-10	6.60E-07	4.34E-10	6.60E-07
4_3							6E-03	4.34E-10	3.32E-07	4.34E-10	3.32E-07
4_4							9E-03	4.33E-10	2.22E-07	4.33E-10	2.22E-07
5_0							0	3.12E-09	1.76E-05	3.12E-09	1.76E-05
5_1							1E-03	3.12E-09	1.80E-06	3.12E-09	1.80E-06
5_2	3E8	2E7	5E4	1E4	5E8	5E8	3E-03	3.11E-09	6.42E-07	3.11E-09	6.42E-07
5_3							6E-03	3.10E-09	3.27E-07	3.10E-09	3.27E-07
5_4							9E-03	3.08E-09	2.19E-07	3.08E-09	2.19E-07

Table S1 continued

exp	$k_{S1\rightarrow S0}$ / s^{-1}	k_{isc} / s^{-1}	k_{risc} / s^{-1}	$k_{T1\rightarrow S0}$ / s^{-1}	k_{qS} / $s^{-1}M^{-1}$	k_{qT} / $s^{-1}M^{-1}$	[Q] / M	τ_{1S} / s	τ_{2S} / s	τ_{1T} / s	τ_{2T} / s
6_0							0	2E-09	3.23E-06	2E-09	3.23E-06
6_1							1E-03	2E-09	1.24E-06	2E-09	1.24E-06
6_2	3E8	2E8	5E5	1E4	5E8	5E8	3E-03	1.99E-09	5.53E-07	1.99E-09	5.53E-07
6_3							6E-03	1.99E-09	3.02E-07	1.99E-09	3.02E-07
6_4							9E-03	1.98E-09	2.08E-07	1.98E-09	2.08E-07
7_0							0	2E-09	7.69E-05	2E-09	7.69E-05
7_1							1E-03	2E-09	1.95E-06	1.99E-09	1.95E-06
7_2	3E8	2E8	5E3	1E4	5E8	5E8	3E-03	1.99E-09	6.61E-07	1.99E-09	6.61E-07
7_3							6E-03	1.99E-09	3.32E-07	1.99E-09	3.32E-07
7_4							9E-03	1.98E-09	2.22E-07	1.98E-09	2.22E-07
8_0							0	2E-09	7.69E-06	2E-09	7.69E-06
8_1							1E-03	2E-09	1.59E-06	2E-09	1.59E-06
8_2	3E8	2E8	5E4	1E5	5E8	5E8	3E-03	1.99E-09	6.14E-07	1.99E-09	6.14E-07
8_3							6E-03	1.99E-09	3.20E-07	1.99E-09	3.20E-07
8_4							9E-03	1.98E-09	2.16E-07	1.98E-09	2.16E-07
9_0							0	2E-09	3.23E-05	2E-09	3.23E-05
9_1							1E-03	2E-09	1.89E-06	2E-09	1.89E-06
9_2	3E8	2E8	5E4	1E3	5E8	5E8	3E-03	1.99E-09	6.54E-07	1.99E-09	6.54E-07
9_3							6E-03	1.99E-09	3.30E-07	1.99E-09	3.30E-07
9_4							9E-03	1.98E-09	2.21E-07	1.98E-09	2.21E-07
10_0							0	2E-09	2.50E-05	2E-09	2.50E-05
10_1							1E-03	1.98E-09	1.85E-06	1.98E-09	1.85E-06
10_2	3E8	2E8	5E4	1E4	5E9	5E8	3E-03	1.94E-09	6.50E-07	1.94E-09	6.50E-07
10_3							6E-03	1.89E-09	3.29E-07	1.89E-09	3.29E-07
10_4							9E-03	1.83E-09	2.20E-07	1.83E-09	2.20E-07
11_0							0	2E-09	2.50E-05	2E-09	2.50E-05
11_1							1E-03	2E-09	1.86E-06	2E-09	1.86E-06
11_2	3E8	2E8	5E4	1E4	5E7	5E8	3E-03	2E-09	6.50E-07	2E-09	6.50E-07
11_3							6E-03	2E-09	3.29E-07	2E-09	3.29E-07
11_4							9E-03	2E-09	2.20E-07	2E-09	2.20E-07
12_0							0	2E-09	2.50E-05	2E-09	2.50E-05
12_1							1E-03	2E-09	1.99E-07	1.99E-09	1.99E-07
12_2	3E8	2E8	5E4	1E4	5E8	5E9	3E-03	1.99E-09	6.65E-08	1.99E-09	6.65E-08
12_3							6E-03	1.99E-09	3.33E-08	1.99E-09	3.33E-08
12_4							9E-03	1.98E-09	2.22E-08	1.98E-09	2.22E-08

Table S1 continued

exp	$k_{S1\rightarrow S0}$ / s^{-1}	k_{isc} / s^{-1}	k_{risc} / s^{-1}	$k_{T1\rightarrow S0}$ / s^{-1}	k_{qS} / $s^{-1}M^{-1}$	k_{qT} / $s^{-1}M^{-1}$	[Q] / M	τ_{1S} / s	τ_{2S} / s	τ_{1T} / s	τ_{2T} / s
13_0							0	2E-09	2.50E-05	2E-09	2.50E-05
13_1							1E-03	2E-09	1.11E-05	2E-09	1.11E-05
13_2	3E8	2E8	5E4	1E4	5E8	5E7	3E-03	1.99E-09	5.26E-06	1.99E-09	5.26E-06
13_3							6E-03	1.99E-09	2.94E-06	1.99E-09	2.94E-06
13_4							9E-03	1.98E-09	2.04E-06	1.98E-09	2.04E-06

S_1 and T_1 energy determination

The E_{00} energies of S_1 and T_1 of **4CzIPN**, **4DPAIPN** and **3DPAFIPN** were obtained from emission spectra recorded at 77 K, exciting samples at 405 nm in a glassy butyronitrile matrix. The E_{00} values were extracted from the emission onset by tangential method, taking the intersection of the tangent at the high energy slope of the peak. [7,8]

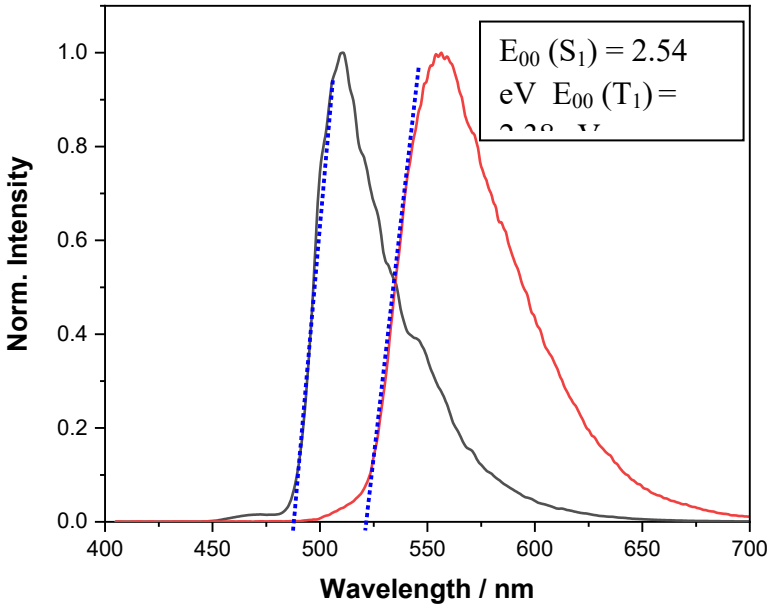

Figure S2: Fluorescence (black line), phosphorescence (red line), tangents at high energy slope (blue dotted lines) of **4DPAIPN** at 77K in butyronitrile matrix; $\lambda_{excitation}$= 405 nm; phosphorescence was acquired with a 7 ms gate and 0.5 ms delay.

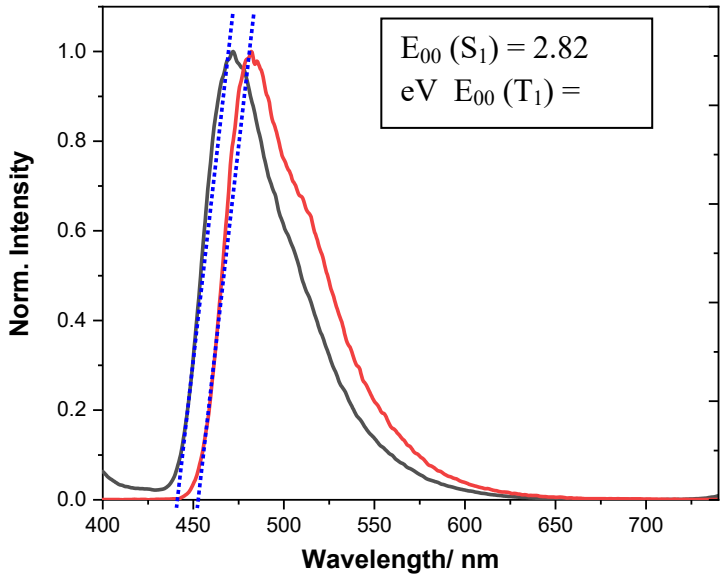

Figure S3: Fluorescence (black line), phosphorescence (red line), tangents at high energy slope (blue dotted lines) of **4CzIPN** at 77K in butyronitrile matrix; $\lambda_{excitation}$= 405 nm; phosphorescence was acquired with a 7 ms gate and 0.5 ms delay.

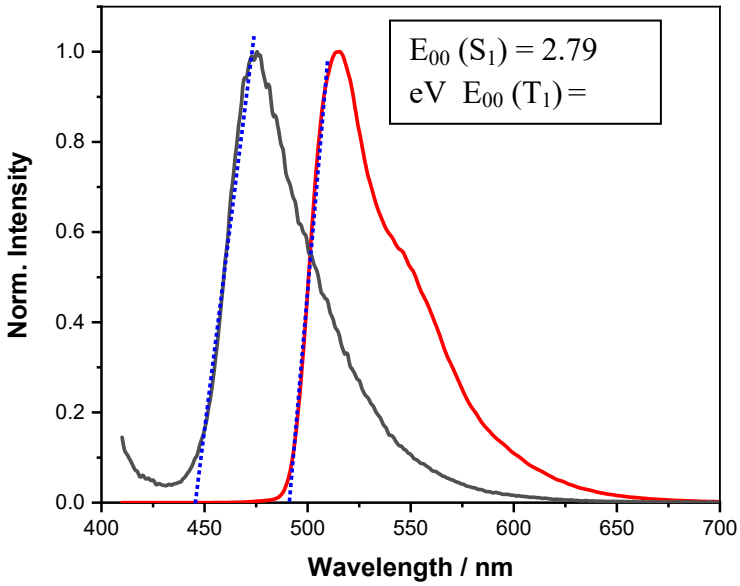

Figure S4: Fluorescence (black line), phosphorescence (red line), tangents at high energy slope (blue dotted lines) of **3DPAFIPN** at 77K in butyronitrile matrix; $\lambda_{excitation}$= 405 nm; phosphorescence was acquired with a 7 ms gate and 0.5 ms delay.

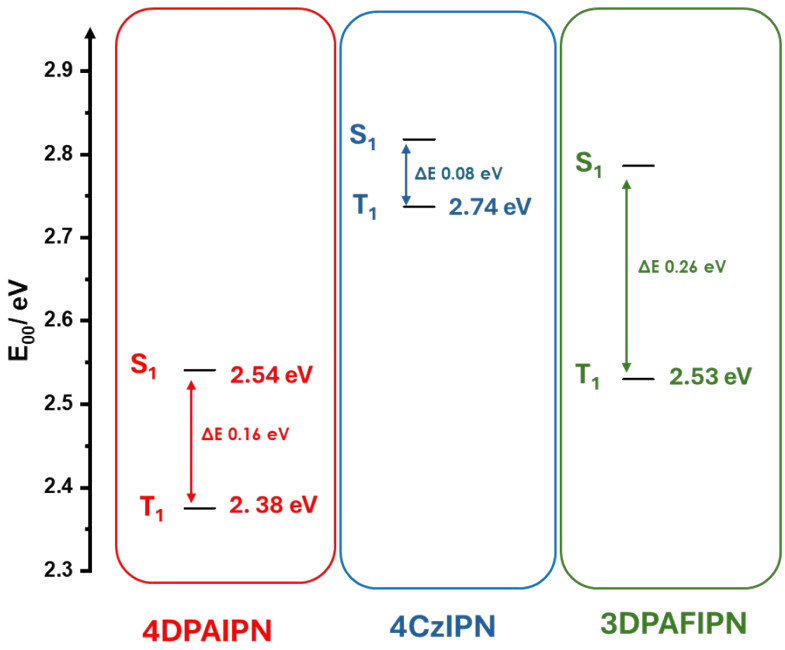

Figure S5: Graphical representation of S_1 and T_1 energies of the TADF photosensitizers and related S_1-T_1 energy gap

Cyclic voltammograms

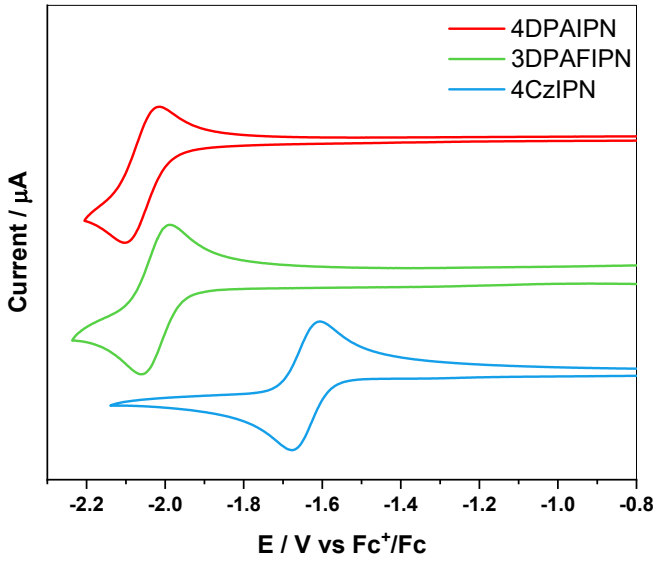

Figure S6: Cyclic voltammograms of TADF photosensitizers (0.5 mM) in dichloromethane solution at room temperature with $TBAPF_6$ 0.1M as supporting electrolyte; scan rate 200 mV·s, glassy carbon as working electrode.

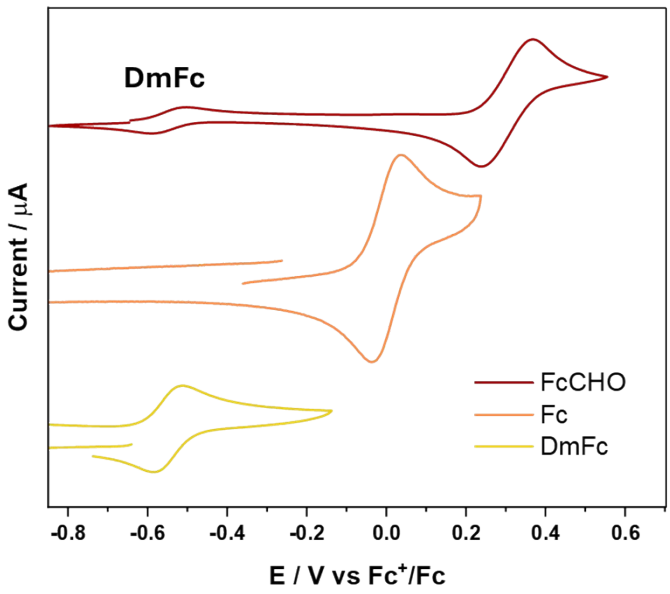

Figure S7: Cyclic voltammograms of ferrocene derivatives (0.5 mM) in dichloromethane solution at room temperature with $TBAPF_6$ 0.1M as supporting electrolyte; scan rate 200 mV·s, glassy carbon as working electrode.

Electronic energy levels of photocatalysts and radical pair

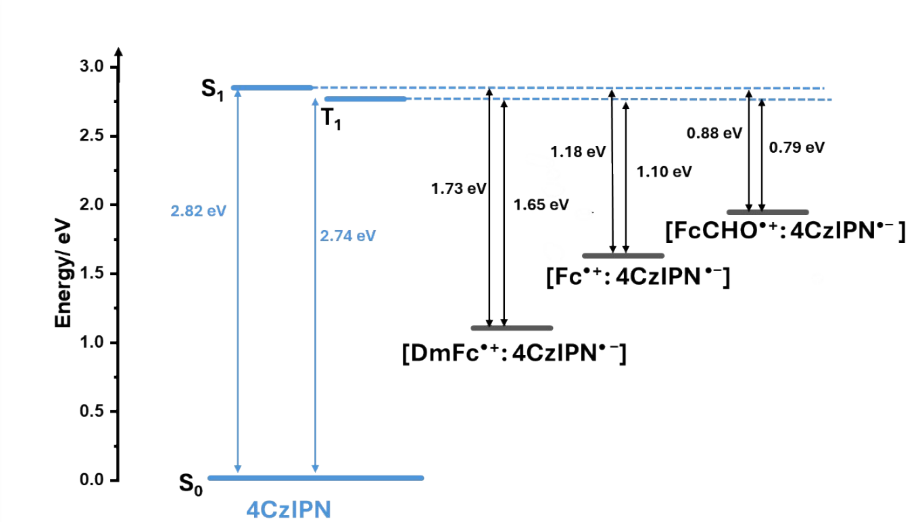

Figure S8: Energy diagram of the relevant electronic states of **4DPAIPN** and of the corresponding radical pairs with ferrocene derivatives produced by photoinduced electron transfers.

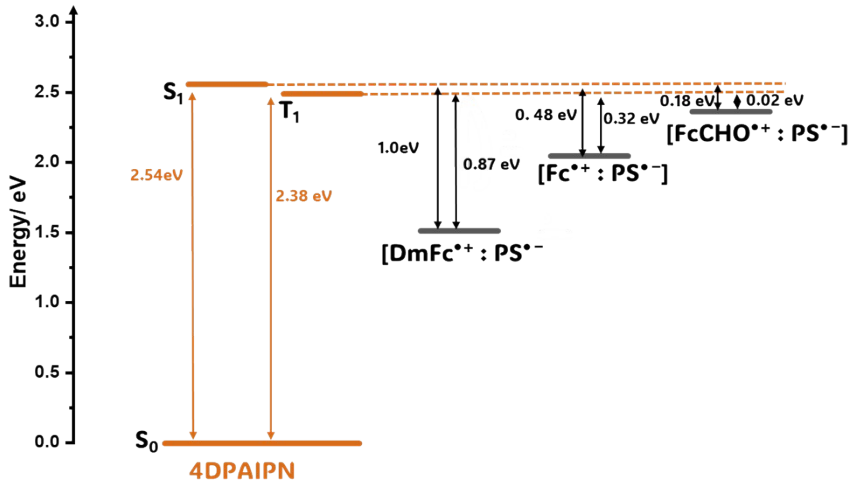

Figure S9: Energy diagram of the relevant electronic states of **4DPAIPN** and of the corresponding radical pairs with ferrocene derivatives produced by photoinduced electron transfers.

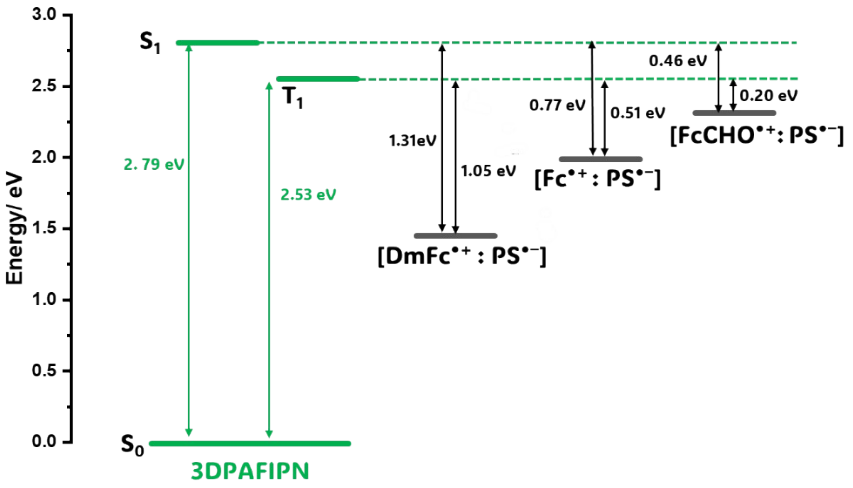

Figure S10: Energy diagram of the relevant electronic states of **3DPAFIPN** and of the corresponding radical pairs with ferrocene derivatives produced by photoinduced electron transfers.

Quenching experiments

Prompt fluorescence quenching studies were performed in air equilibrated toluene solutions, while delayed fluorescence quenching were performed in previously degassed toluene, and solutions were prepared in a glove box. Each component of fluorescence time decay was individually fitted with a single exponential function.

The photoinduced electron transfer between the excited state (S_1 or T_1) of the TADF photosensitiser (*S) and the quencher Q can be expressed by the following processes:

$$*S + Q \underset{k_{-d}}{\overset{k_d}{\rightleftharpoons}} *S.Q \xrightarrow{k_{el.tr.}} S^{\bullet-}.Q^{\bullet+} \xrightarrow{k'_{-d}} S^{\bullet-} + Q^{\bullet+}$$

Under the steady-state approximation, i.e. [*S.Q] constant over time, the observed rate constant k_{obs} is given by the following equation:

$$k_{obs} = k_d \frac{k_{el.tr.}}{k_{el.tr.} + k_{-d}}$$

When $k_{el.tr.} >> k_{-d}$ the observed rate constant is the diffusion constant k_d.

The (observed) quenching constants, from now on referred to as k_q for prompt or delayed fluorescence were obtained by fitting experimental points according to Stern-Volmer equation:

$$\frac{\tau^0}{\tau} = 1 + k_q \tau^0 [Q]$$

where τ^0 and τ are the fluorescence lifetime in absence and presence of a quencher Q, respectively.

Quenching with DIPEA

4DPAIPN

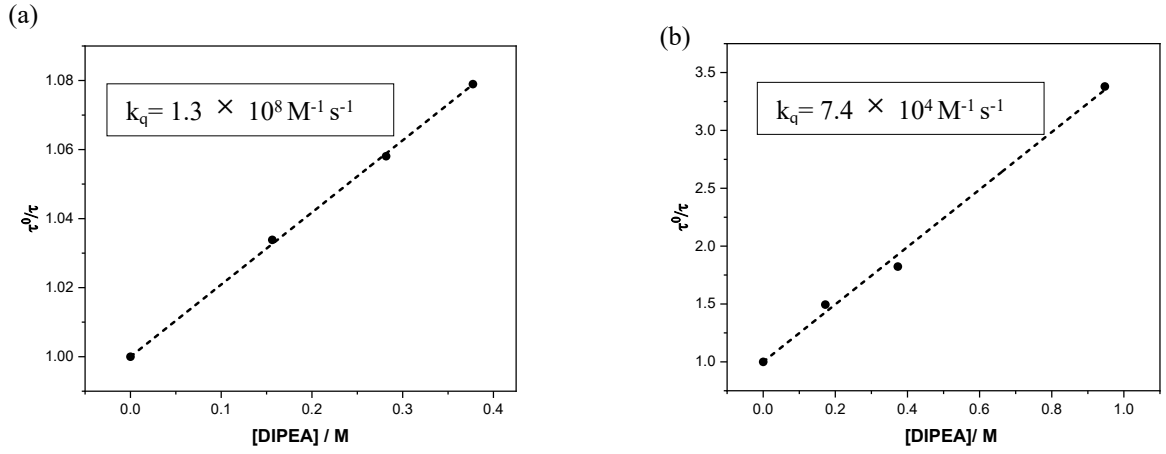

Figure S11: Stern-Volmer plots of **4DPAIPN** (0.1 mM) with **DIPEA** as quencher for (a) prompt fluorescence measured in air-equilibrated toluene and (b) delayed fluorescence measured in deaerated toluene.

4CzIPN

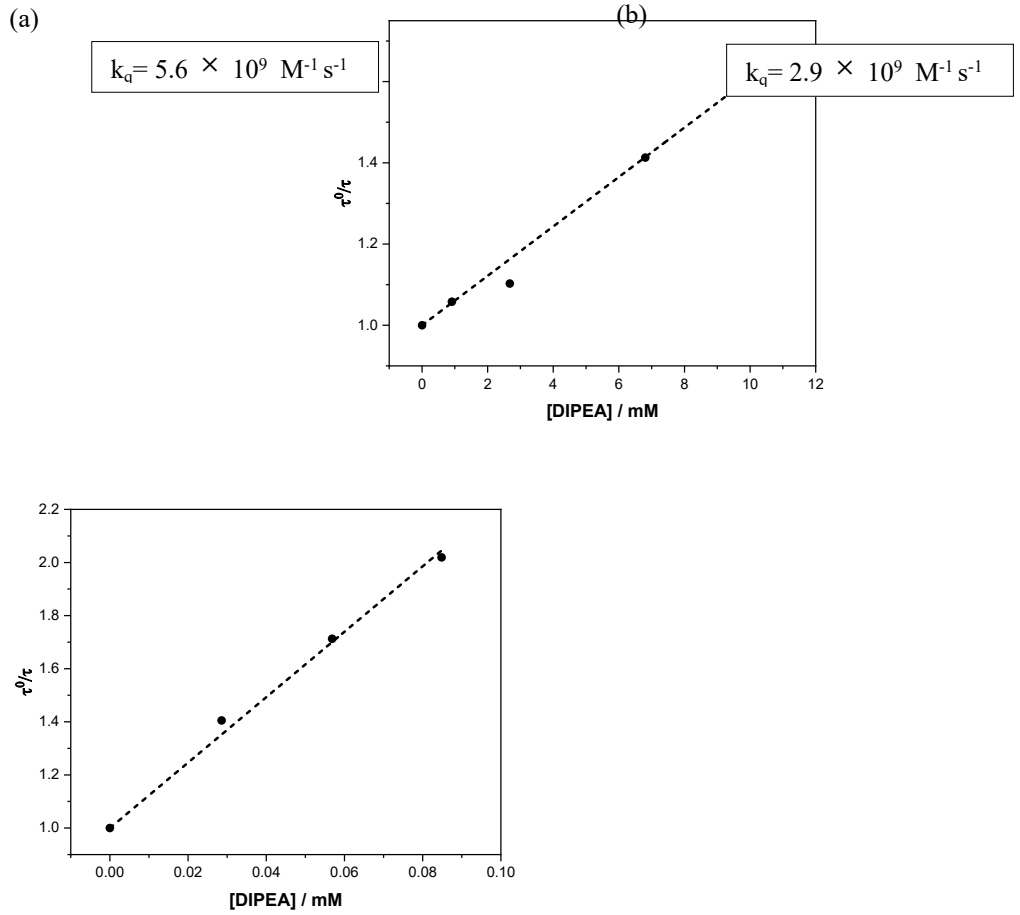

Figure S12: Stern-Volmer plots of **4CzIPN** (0.1 mM) with **DIPEA** as quencher for (a) prompt fluorescence measured in air-equilibrated toluene and (b) delayed fluorescence measured in deaerated toluene.

3DPAFIPN

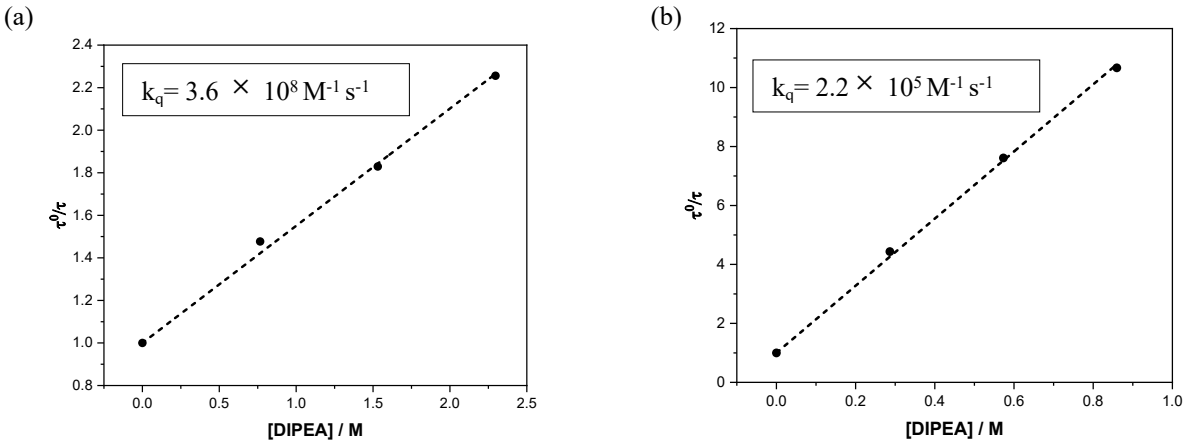

Figure S13: Stern-Volmer plots of **3DPAFIPN** (0.1 mM) with **DIPEA** as quencher for (a) prompt fluorescence measured in air-equilibrated toluene and (b) delayed fluorescence measured in deaerated toluene.

Quenching with ferrocene derivatives

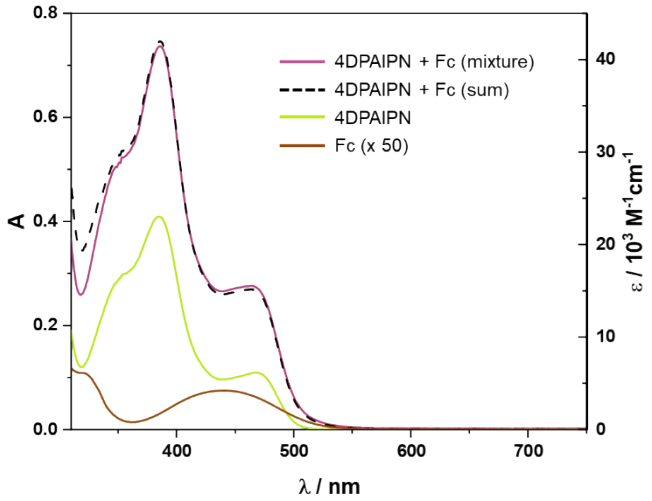

Figure S14: Absorption spectra of the mixture (solid purple line) and the sum (dash black line) of **4DPAIPN** (30 μM) + **Ferrocene** (1.3 mM) in toluene. The sum spectrum is calculated based on the spectra of the isolated compounds and their concentrations. For comparison, the spectra in ε of the isolated compounds in the same solvent are reported (brown and green solid lines).

Upon mixing **4DPAIPN** and **Ferrocene**, the absorption spectrum of the solution is equivalent to the sum of the spectra of the isolated compounds (Figure S14). This evidence indicates that there is no interaction at the ground state between the photosensitizer and the quencher, excluding the possibility of static quenching. Given the very similar structures of the photosensitizers considered in this study and the quenchers chosen, we can safely assume that for all the couples PS/Q considered in this study we observe only dynamic quenching.

4DPAIPN

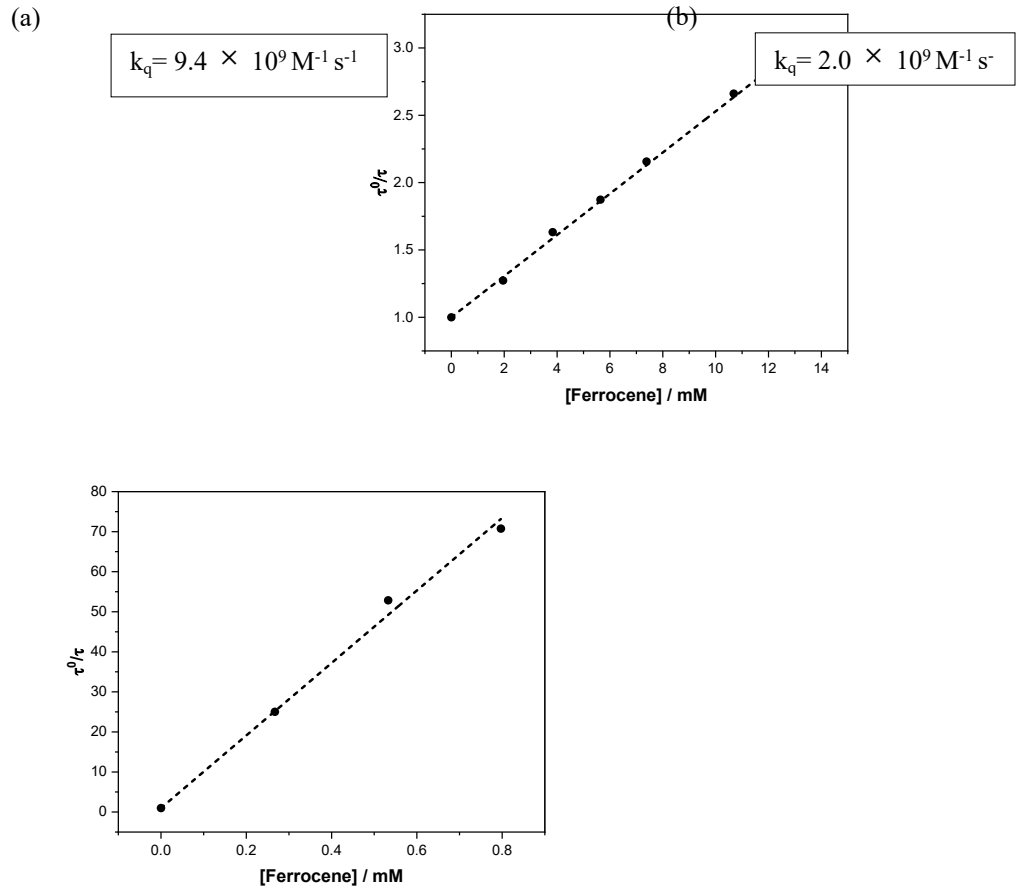

Figure S15: Stern-Volmer plots of **4DPAIPN** (0.1 mM) with **ferrocene** as quencher for (a) prompt fluorescence measured in air-equilibrated toluene and (b) delayed fluorescence measured in deaerated toluene.

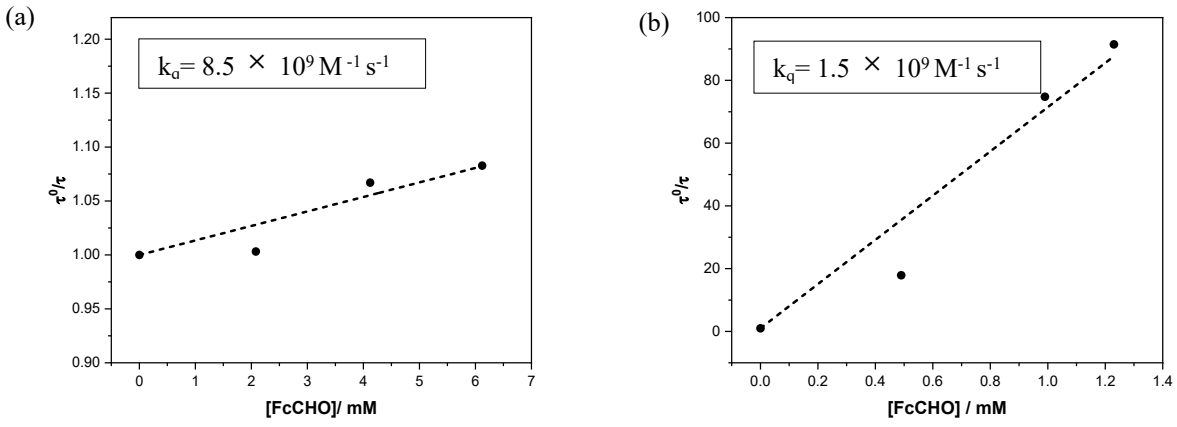

Figure S16: Stern-Volmer plots of **4DPAIPN** (0.1 mM) with **ferrocenecarboxyaldheyde** as quencher for (a) prompt fluorescence measured in air-equilibrated toluene and (b) delayed fluorescence measured in deaerated toluene.

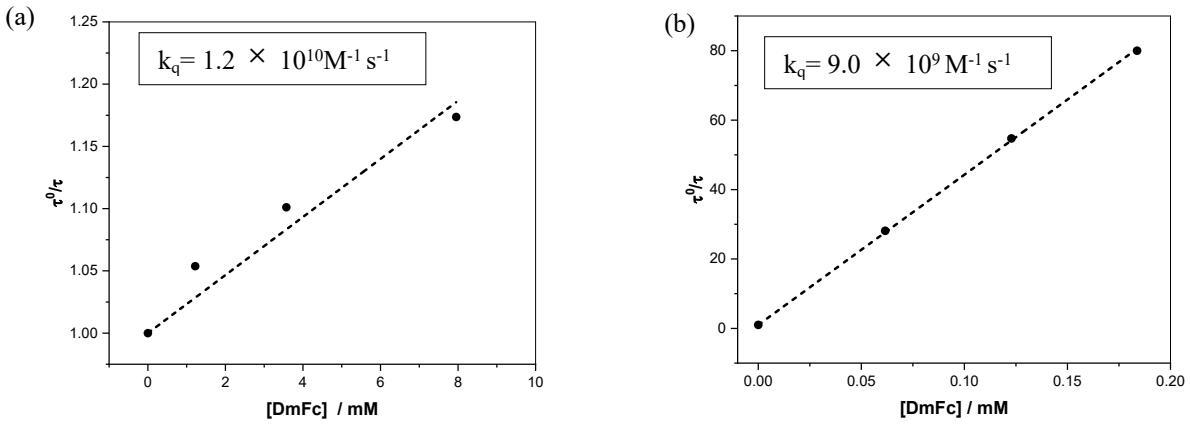

Figure S17: Stern-Volmer plots of **4DPAIPN** (0.1 mM) with **decamethylferrocene** as quencher for (a) prompt fluorescence measured in air-equilibrated toluene and (b) delayed fluorescence measured in deaerated toluene.

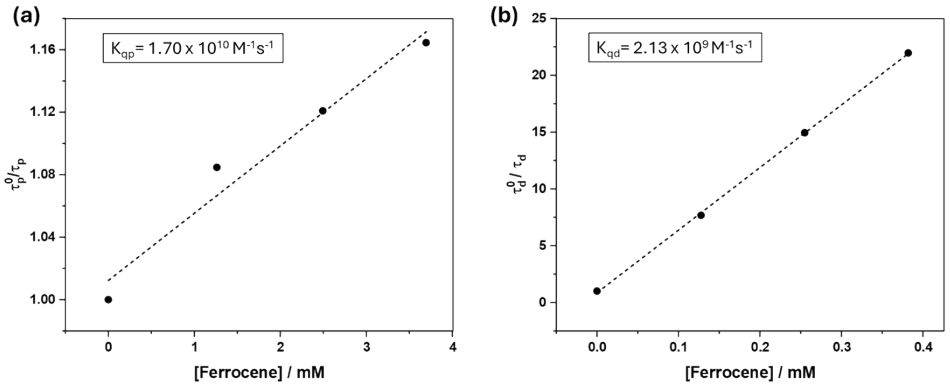

Figure S18: Stern-Volmer plots of **4DPAIPN** (0.1 mM) with **ferrocene** as quencher for (a) prompt fluorescence measured in air-equilibrated $CHCl_2$ and (b) delayed fluorescence measured in deaerated $CHCl_2$.

4CzIPN

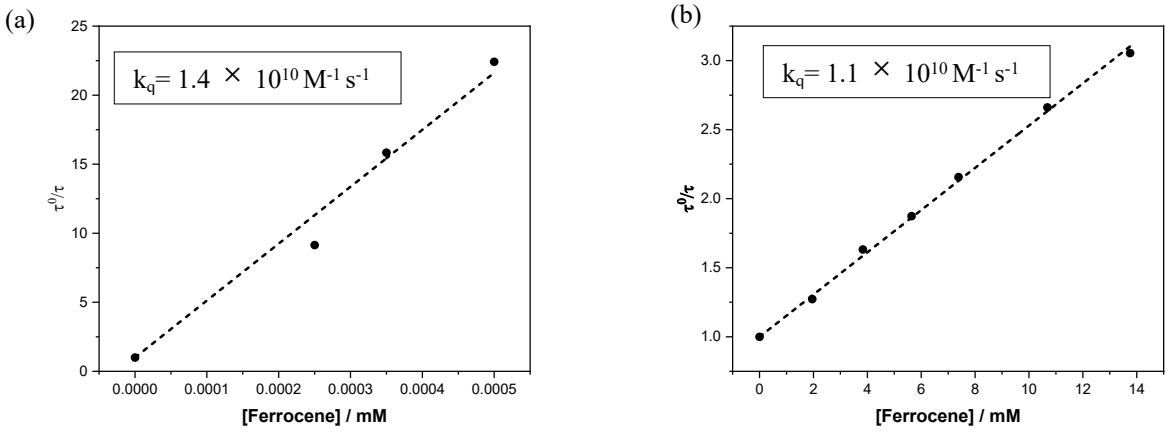

Figure S19: Stern-Volmer plots of **4CzIPN** (0.1 mM) with **ferrocene** as quencher for (a) prompt fluorescence measured in air-equilibrated toluene and (b) delayed fluorescence measured in deaerated toluene.

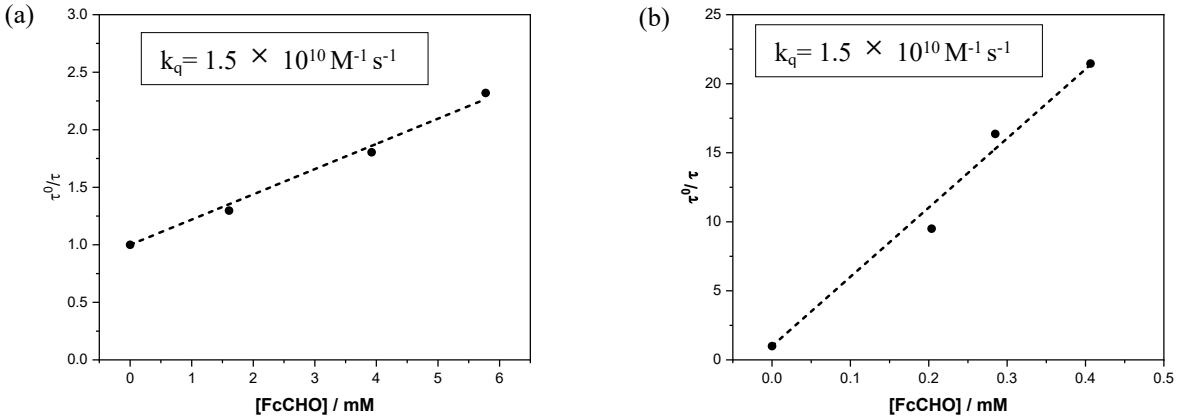

Figure S20: Stern-Volmer plots of **4CzIPN** (0.1 mM) with **ferrocenecarboxyaldheyde** as quencher for (a) prompt fluorescence measured in air-equilibrated toluene and (b) delayed fluorescence measured in deaerated toluene.

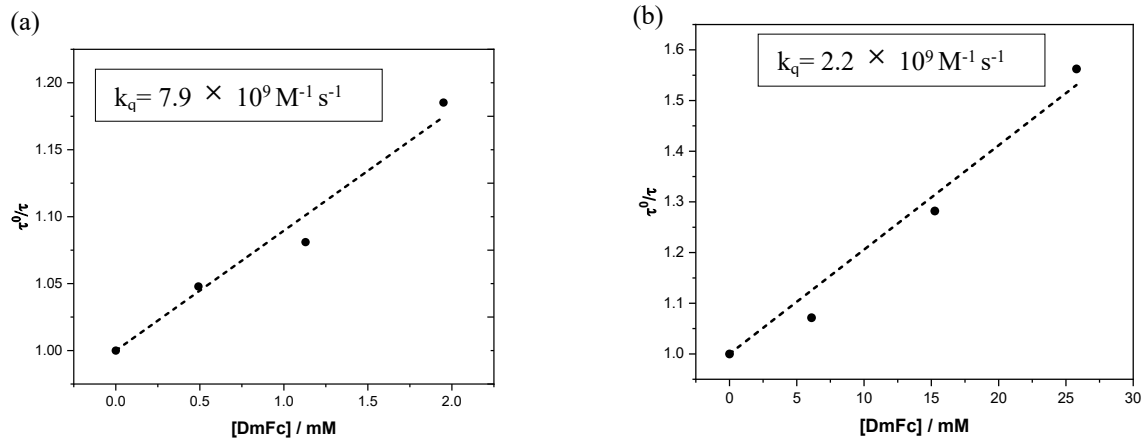

Figure S21: Stern-Volmer plots of **4CzIPN** (0.1 mM) with **decamethylferrocene** as quencher for (a) prompt fluorescence measured in air-equilibrated toluene and (b) delayed fluorescence measured in deaerated toluene.

3DPAFIPN

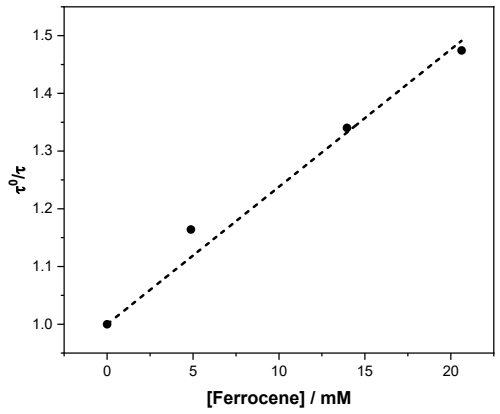

(a)

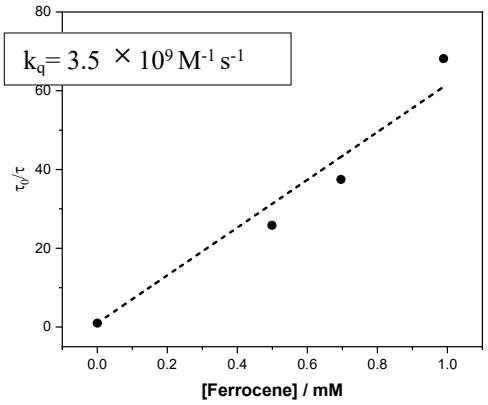

(b)

k_q= 8.1 × 10^8 M^{-1} s^{-1}

Figure S22: Stern-Volmer plots of **3DPAFIPN** (0.1 mM) with **ferrocene** as quencher for (a) prompt fluorescence measured in air-equilibrated toluene and (b) delayed fluorescence measured in deaerated toluene.

(a)

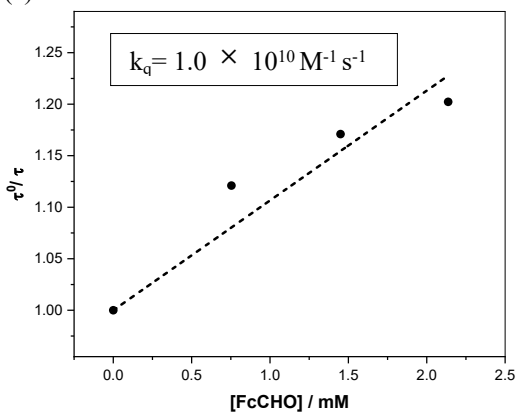

(b)

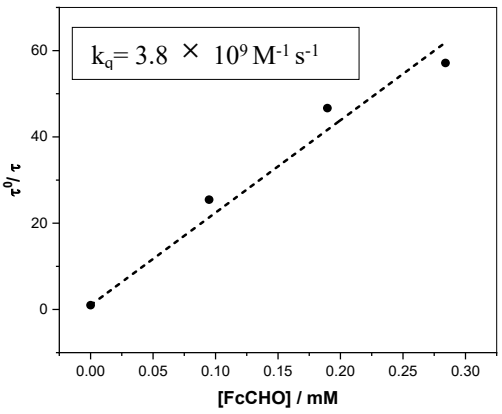

Figure S23: Stern-Volmer plots of **3DPAFIPN** (0.1 mM) with **ferrocenecarboxyaldheyde** as quencher for (a) prompt fluorescence measured in air-equilibrated toluene and (b) delayed fluorescence measured in deaerated toluene.

(a)

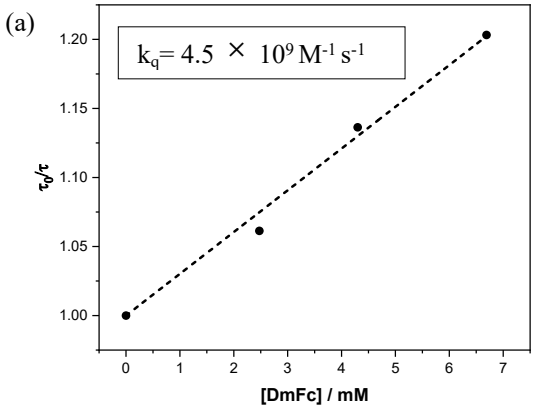

(b)

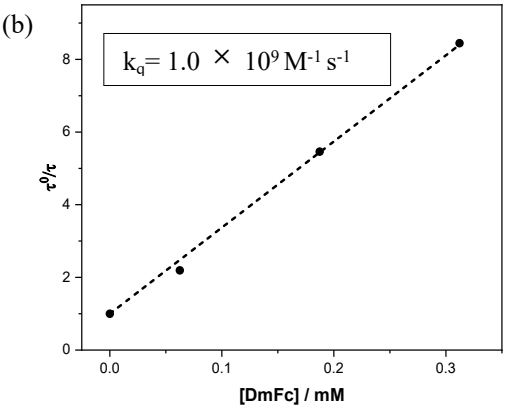

Figure S24: Stern-Volmer plots of **3DPAFIPN** (0.1 mM) with **decamethylferrocene** as quencher for (a) prompt fluorescence measured in air-equilibrated toluene and (b) delayed fluorescence measured in deaerated toluene

Quenching with naphthoquinone derivatives

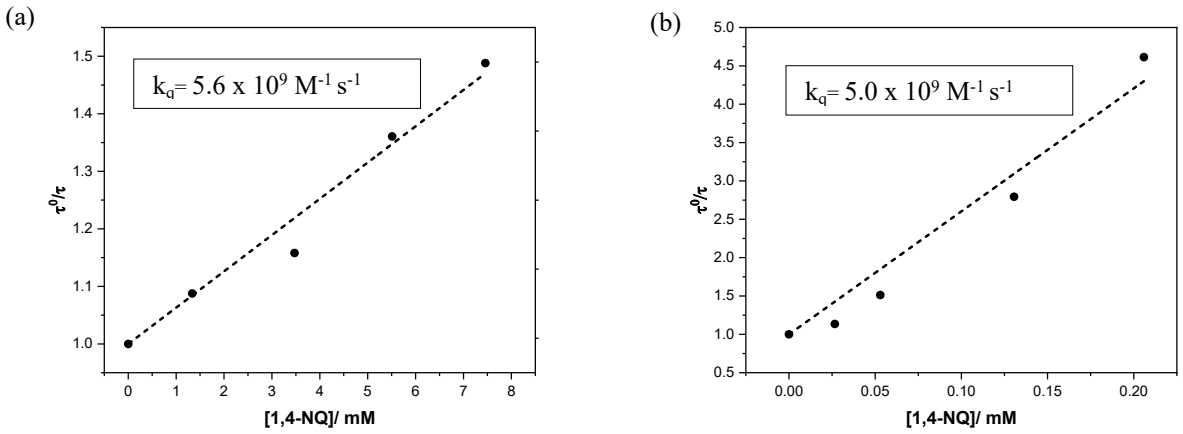

Figure S25: Stern-Volmer plots of **4CzIPN** (0.1 mM) with **napthoquinone** as quencher for (a) prompt fluorescence measured in air-equilibrated toluene and (b) delayed fluorescence measured in deaerated toluene

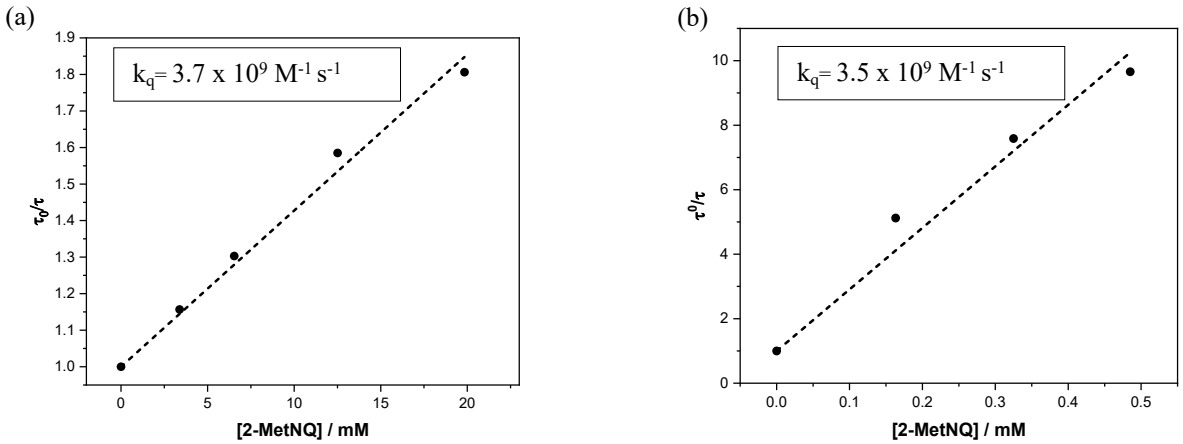

Figure S26: Stern-Volmer plots of **4CzIPN** (0.1 mM) with **2-methylnapthoquinone** as quencher for (a) prompt fluorescence measured in air-equilibrated toluene and (b) delayed fluorescence measured in deaerated toluene .

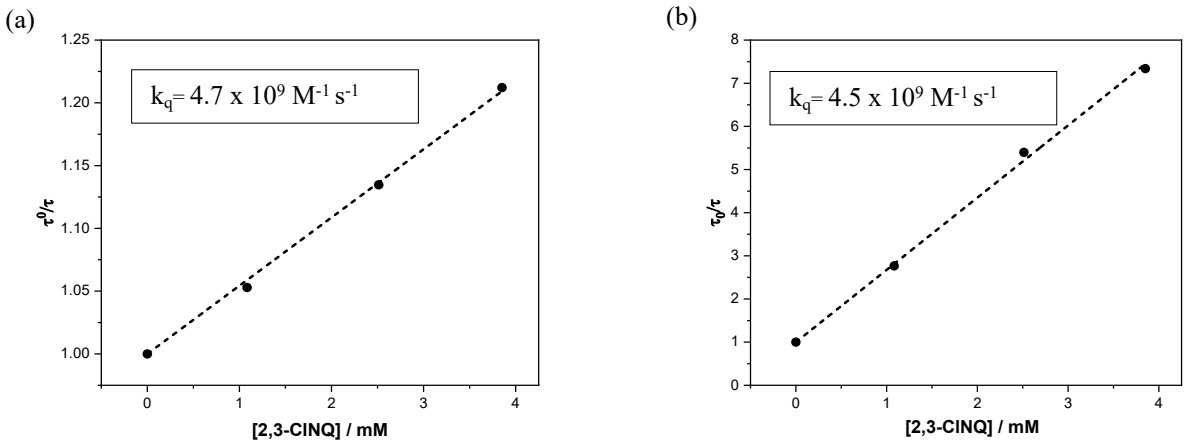

Figure S27: Stern-Volmer plots of **4CzIPN** (0.1 mM) with **2,3-dichloronaphthoquinone** as quencher for (a) prompt fluorescence measured in air-equilibrated toluene and (b) delayed fluorescence measured in deaerated toluene

Rehm-Weller plot for ferrocene derivatives with TADF photosensitizers

The relationship between the free energy and the rate constant of photoinduced electron transfer (ΔG) is given by the equation:

$$k_{el} = \nu_N \kappa_{el} e^{-\frac{\Delta G^{\neq}}{RT}}$$

where ν_N is the average nuclear frequency factor, κ_{el} is the electronic transmission coefficient, and $\Delta G^{\neq}$ is the activation free energy, expressed by the Marcus relationship:[12]

$$\Delta G^{\neq} = \frac{1}{4\lambda}(\Delta G^0 + \lambda)^2$$

where ΔG^0 is the standard free energy change of the reaction and λ is the nuclear reorganizational energy.

The structural similarity among the ferrocene-based quenchers used in our experiments as well as the similarity among the TADF photosensitizers suggests that the steric and electronic factors for the respective reactions were similar, and therefore, that the experimental quenching constants were proportional to k_{el}. Thus, plotting $\log(k_q)$ as a function of ΔG^0 should represent the shape of the Rehm-Weller plot, $\log(k_{el})$ vs ΔG_0.

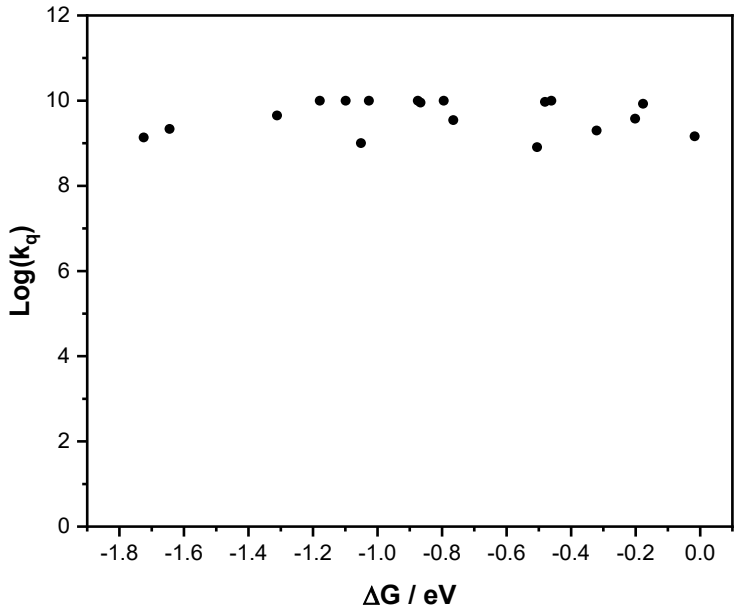

Figure S28: Rehm-Weller-like plot based on the quenching experiments employing either prompt or delayed fluorescence of TADF photosensitizers and ferrocene derivatives. The shape of the plot does not follow the Marcus equation, supporting the notion that the differences between the observed k_qS and k_qT are not due to the differences in the PET driving forces only.

Computational data

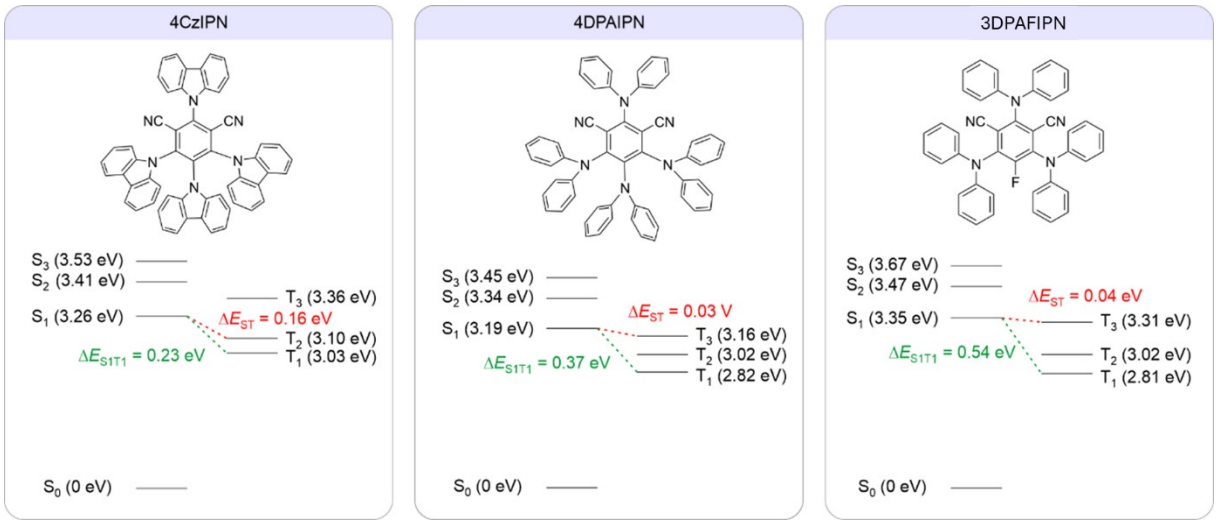

Figure S29: Energy level of vertical singlet excited and triplet excited states of **4CzIPN**, **4DPAIPN**, and **3DPAFIPN**.

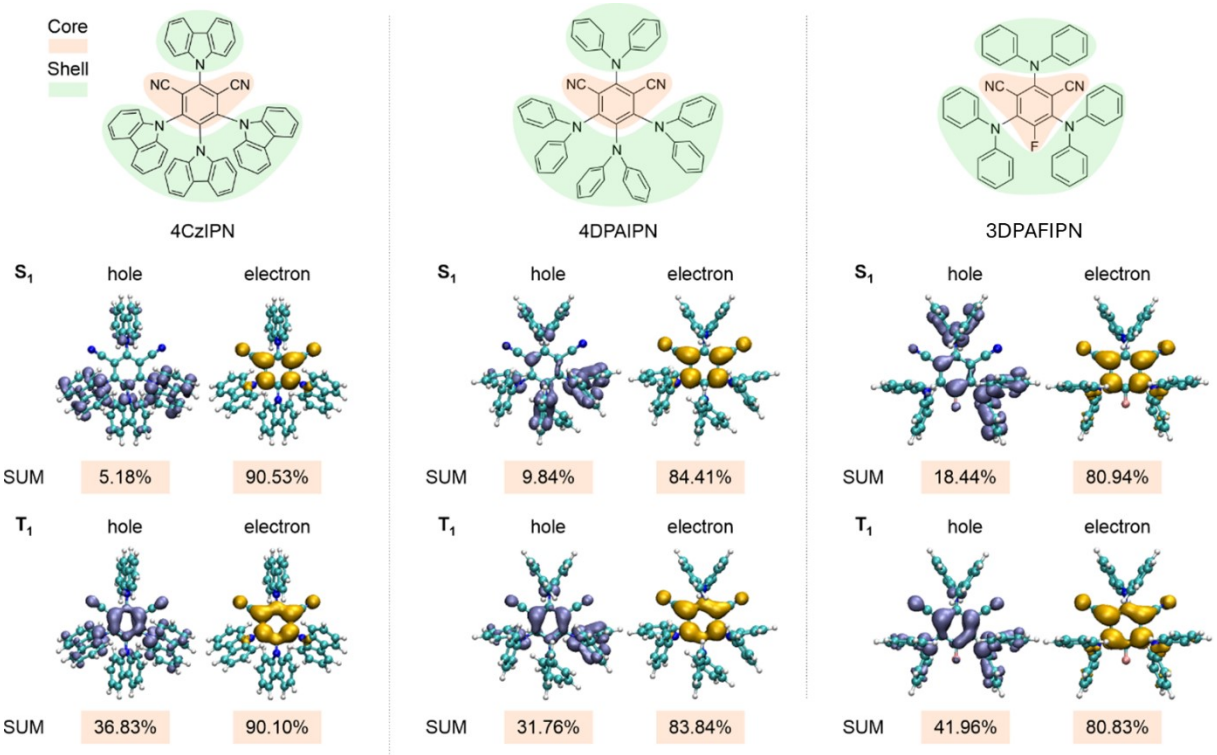

Figure S30: Fragments contribution of the "core" on hole or electron distribution of **4CzIPN**, **4DPAIPN**, and **3DPAFIPN** in vertical S_1 and T_1 states.

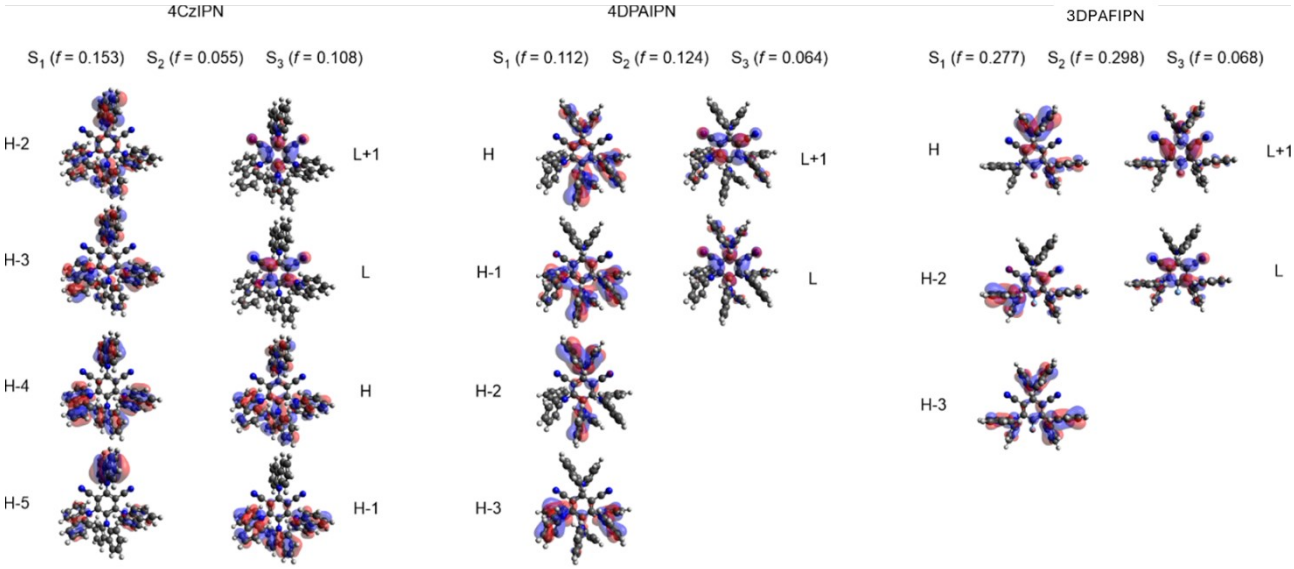

Figure S31: The molecule orbitals of vertical excited singlet states with oscillator strength of **4CzIPN**, **4DPAIPN**, and **3DPAFIPN**. H means the highest occupied molecular orbital (HOMO) and L means the lowest unoccupied molecular orbital (LUMO).

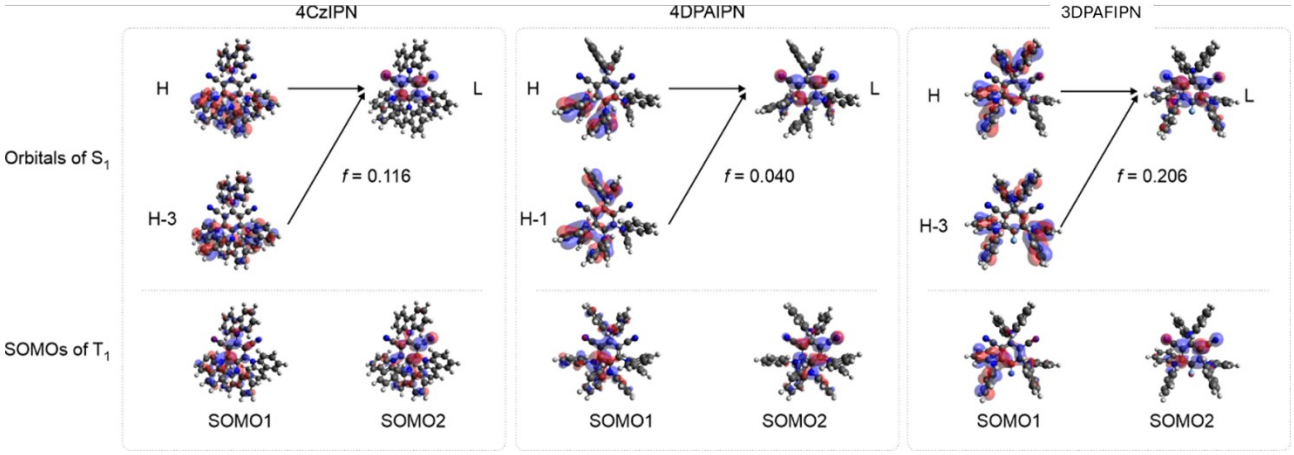

Figure S32: The molecule orbitals of adiabatic S_1 and T_1 states with oscillator strength of **4CzIPN**, **4DPAIPN**, and **3DPAFIPN**. The SOMOs are the singly occupied molecular orbitals calculated by UDFT.

References

1. Frisch, M. J.; Trucks, G. W.; Schlegel, H. B.; Scuseria, G. E.; Robb, M. A.; Cheeseman, J. R.; Scalmani, G.; Barone, V.; Petersson, G. A.; Nakatsuji, H.; Li, X.; Caricato, M.; Marenich, A. V.; Bloino, J.; Janesko, B. G.; Gomperts, R.; Mennucci, B.; Hratchian, H. P.; Ortiz, J. V.; Izmaylov, A. F.; Sonnenberg, J. L.; Williams, D.; Ding, F.; Lipparini, F.; Egidi, F.; Goings, J.; Peng, B.; Petrone, A.; Henderson, T.; Ranasinghe, D.; Zakrzewski, V. G.; Gao, J.; Rega, N.; Zheng, G.; Liang, W.; Hada, M.; Ehara, M.; Toyota, K.; Fukuda, R.; Hasegawa, J.; Ishida, M.; Nakajima, T.; Honda, Y.; Kitao, O.; Nakai, H.; Vreven, T.; Throssell, K.; Montgomery Jr., J. A.; Peralta, J. E.; Ogliaro, F.; Bearpark, M. J.; Heyd, J. J.; Brothers, E. N.; Kudin, K. N.; Staroverov, V. N.; Keith, T. A.; Kobayashi, R.; Normand, J.; Raghavachari, K.; Rendell, A. P.; Burant, J. C.; Iyengar, S. S.; Tomasi, J.; Cossi, M.; Millam, J. M.; Klene, M.; Adamo, C.; Cammi, R.; Ochterski, J. W.; Martin, R. L.; Morokuma, K.; Farkas, O.; Foresman, J. B.; Fox, D. J. *Gaussian 16 Rev. C.01*, Gaussian, Inc., Wallingford CT: Wallingford, CT, **2016**.
2. Ö. H. Omar, T. Nematiaram, A. Troisi, D. Padula, *Sci. Data* **2022,** *9* (1), 54.
3. Y. Zhao, D. G. Truhlar, *Theor. Chem. Acc.* **2008,** *120* (1), 215-241.
4. E. Cancès, B. Mennucci, J. Tomasi, *The Journal of Chemical Physics* **1997,** *107* (8), 3032-3041
5. M. Villa, A. Fermi, F. Calogero, X. Wu, A. Gualandi, P. G. Cozzi, A. Troisi, B. Ventura, P. Ceroni, C*hemical Science* **2024,** *15* (36), 14739-14745
6. T. Lu, F. Chen, J. *Comput. Chem.* **2012,** *33* (5), 580-592
7. J. Gierschner, J. Cornil, H.J. Egelhaaf, Advanced *Materials,* **2007,** *19*, 173–191
8. Y. Kwon, J. Lee, Y. Noh, D. Kim, Y. Lee, C. Yu, J. C. Roldao, S. Feng, J. Gierschner, R. Wannemacher, M. S. Kwon, *Nat Commun* **2023**, *14* (1)